DOWNSCALING CLIMATE PROJECTIONS TO MODEL ECOLOGICAL CHANGE ON TOPOGRAPHICALLY DIVERSE LANDSCAPES OF THE ARID SOUTHWESTERN UNITED STATES.

Gregg M. Garfin[1], Jon K. Eischeid[2], Melanie Lenart[1], Kenneth L. Cole[3], Kirsten Ironside[4], and Neil Cobb[5].

[1]Institute of the Environment, University of Arizona, 715 N. Park Ave., 2nd Fl., Tucson, AZ 85719; gmgarfin@email.arizona.edu

[2]NOAA Earth Systems Research Laboratory, 325 Broadway, Boulder, CO 80305; jon.k.eischeid@noaa.gov

[3]USGS Southwest Biological Science Center, Colorado Plateau Research Station, P.O. Box 5614, Northern Arizona University, Flagstaff, AZ 86011; ken_cole@usgs.gov

[4]Environmental Sciences and Public Policy Program, Northern Arizona University, P.O. Box 6077, Flagstaff, AZ 86011; Kirsten.Ironside@nau.edu

[5]Merriam-Powell Center for Environmental Research, Northern Arizona University, Flagstaff, AZ 86011; Neil.Cobb@nau.edu

Abstract. Recent and rapid forest mortality in western North America and associated changes in fire frequency and area burned are among the chief concerns of ecosystem managers. These examples of climate change surprises demonstrate nonlinear and threshold ecosystem responses to increased temperatures and severe drought. Given these changes, ecosystem managers in the southwestern United States consistently request

region-specific estimates of climate and vegetation change, in order to provide guidance for management of federal and state forest, range, and riparian ecosystems. In order to help address this need, we developed downscaled climate projections for the Southern Colorado Plateau (SCP: 35°-38°N, 114°-107°W), centered on the Four Corners states. We selected five of twenty-two global climate models (GCMs) from the archive of model runs used in the Intergovernmental Panel on Climate Change Fourth Assessment Report. We based our model selection on GCM simulations of observed critical seasonality for vegetation in the SCP. We used three key seasons in our analysis, winter (November-March), arid foresummer (May-June), and monsoon (July-September). We statistically downscaled projections of temperature and precipitation to a 4 km grid. Projections for the SCP describe a warmer future, in which annual temperatures seem likely to increase by 1.5°-3.6°C by mid-century, and 2.5°-5.4°C by the end of the century, depending on the model chosen. Annual temperatures are projected to exceed the 1950-1999 range of variability by the 2030s. Annual precipitation changes are more equivocal. A conservative estimate, using a 22-model ensemble average, indicates that SCP annual precipitation may decrease by 6% by the end of the century. The least equivocal precipitation projection shows SCP May-June arid foresummer precipitation declining, by 11-45% during the 21st century. Decreasing spring precipitation and substantially increasing temperatures increase the likelihood of further episodes of forest dieback during the 21st century.

Key words: downscaling, climate change, vegetation change modeling, Southern Colorado Plateau

1. Introduction

Between 2000-2004, the USDA Forest Service estimates that nearly 1.4 million hectares of forest land (about 60% in piñon-juniper and the rest in ponderosa pine) in the southwestern U.S. were impacted by mortality (USDA, 2008). This recent and rapid pine mortality in the southwestern United States (Shaw et al., 2005) has raised concern among land managers regarding the potential impacts of severe sustained drought and climate change on southwestern ecosystems. Research on pinyon pine mortality in the Southern Colorado Plateau suggests that a combination of drought and unusually high temperatures depleted soil moisture to a greater extent than during past drought episodes, thus exposing trees to "global-change-style" drought stress (Adams et al., 2009; Breshears et al., 2005). Moreover, researchers speculate that increasing temperatures also enhance insect life cycles and predispose southwestern forests to greater risk of massive mortality in response to drought (Stephenson et al., 2006; Burkett et al., 2005; Logan et al., 2003). Concerns about massive and abrupt changes to southwestern ecosystems are reinforced by observed and projected regional climate changes, which include earlier bud break and flowering (Cayan et al., 2001), enhanced disturbance regimes (Westerling et al., 2006), changes to winter precipitation and snowmelt (Knowles et al., 2006; Stewart et al., 2005), increased occurrence of climate and weather extremes (CCSP, 2008b; Seager et al., 2007; Diffenbaugh et al; 2005; Meehl et al., 2004). Changes in climate may alter the distribution and abundance of species through local-to-regional extinctions, migration, and adaptation to new climates. Given the variety of plausible changes and their

ramifications for ecosystem function, erosion, and land management agency mission goals, managers require credible estimates of future vegetation and ecosystem changes.

The primary climatic variables affecting the distribution of plant species in the area are minimum temperature and seasonal moisture availability (Thompson et al., 1998). Moisture availability is a compound result of temperature, precipitation, and humidity; thus, modeling the relationship between climate and vegetation within arid regions can be complex, involving seasonal changes in multiple variables. In arid regions, such as the Southern Colorado Plateau (SCP; Figure 1), minor declines in total precipitation, small increases in precipitation variability, or seasonal shifts in precipitation, can have sizeable effects on vegetation. If combined with even minor increases in temperature, the impacts on vegetation can be extensive.

Climate has long been known to be important in determining the distribution of native plants on the landscape. The physiological adaptations of individual plant species allow them to take advantage of seasonal patterns in available moisture. Topographic diversity within Northern Arizona creates several vegetation life zones within the region. Temperature and precipitation can vary greatly from the lower regions of the Grand Canyon to the top of the San Francisco Peaks, but the seasonality of these parameters is the same, regardless of altitude, slope, and aspect. Annual precipitation follows a bimodal distribution, split between large, spatially coherent, winter frontal storms and isolated summer monsoon convective storms.

Moisture surplus in the SCP typically occurs from November to March (Figure 2). April reflects a turning point when monthly mean temperatures rise to a point where the growing season typically begins even as precipitation decreases. By May and June, temperatures rise high enough to affect water vapor pressure. The typically sparse rainfall does little to offset high levels of potential evapotranspiration (PE). This period of time can cause severe vegetation stress and even mortality in seedlings lacking an established root system and, during extreme years, in established perennial species (Breshears et al., 2005). Many of the perennial bunch grasses common to northern Arizona remain semi-dormant during this time period. For woody plant recruitment, this is often a critical period; ponderosa pine (*Pinus ponderosa)*, the dominant tree in the region, has been shown to have had cohort events occurring during anomalously cool and wet May-June periods (Savage et al., 1996). Conversely, ponderosa forests are most susceptible to damage from bark beetle infestation and wildfires when these pre-monsoon months are anomolously dry (Adams et al., 2009).

On average, Southern Colorado Plateau summer monsoon precipitation begins in mid-July (Higgins et al., 1999). Although it occurs during a time when PE and average monthly temperature are at their annual peaks, it typically brings enough precipitation to decrease the moisture deficit during this time of year (Figure 2). As average monthly temperature begins to decrease in August, monsoon precipitation reaches its regional apex, which further decreases the moisture deficit. By mid-September, monsoon precipitation typically decreases, but so does temperature. October, like April, is a transition period between annual moisture surplus and deficit.

Vegetation models can utilize information on sub-seasonal and interannual climate variations, including the moisture balance variations described above, to project future ecosystem change. This can help provide guidance needed by land managers to evaluate management strategies and climate change adaptation options (e.g., Bachelet et al., 2003). Climate change impact studies, using vegetation models, have taken two general approaches: (1) statistically modeling shifts in the distribution of acceptable climate areas (potential habitat) for individual species, and (2) simulating ecosystem processes using vegetation units. The first method has been criticized for not including important ecosystem processes (Bonan et al., 2003; Morin et al., 2008), and the second method has been criticized for not taking into account species-specific responses to change (Rehfeldt et al., 2006). Paleoecological studies have long suggested vegetation shifts of individual species (e.g., Jackson and Overpeck, 2000). Changes have rarely been described as a shift of a classified vegetation association, unless the association is defined by one species.

This paper addresses the initial phase of efforts to model changes in individual plant species distributions on the Southern Colorado Plateau. Vegetation modeling will be applied to data from the 3,000 m elevation gradient from the low deserts of the Grand Canyon to the alpine tundra of the San Francisco Peaks in northern Arizona. This is an area for which we have compiled abundant baseline GIS data as well as information from numerous studies of ongoing ecological changes. We hypothesize that many future disturbance processes influenced by climate such as bark beetle outbreaks, drought mortality, wildfire frequency, and exotic species spread can be simulated using our

climate model results. We describe here the process and results of GCM selection and statistical downscaling of climate parameters for input into process-based landscape-scale vegetation models. In section two, we describe the GCM data, downscaling methods, and model selection criteria. In section three, we discuss the GCMs and ensemble averages selected, and we examine the spatial and temporal fidelity of the GCMs in reproducing the seasonal cycle of temperature and precipitation over the domain of the study region. In section four, we discuss the GCM projections for 21st century over the study domain, and compare our results with projections from other studies. In section five, we evaluate the ecological implications of the projected changes, discuss implications for the vegetation modeling component of the study, and we discuss alternatives to our approach that may inform future studies. Section six contains a summary of major conclusions.

2. Data and Methods

Historic Climate Records

We used mean monthly temperature and monthly total precipitation data from the Parameter-elevation Regressions on Independent Slopes Model (PRISM) 4 km grid cell resolution dataset (Daly et al. 1994) (www.prism.oregonstate.edu). PRISM uses point data, spatial data sets, a knowledge base, and expert interaction to generate estimates of gridded monthly climatic parameters (Daly et al., 2001). A combination of linear regression and a series of rules, decisions and calculations set weights for the station data

entering the linear regression (Daly et al., 2002). The weighting function contains information about relationships between the climate field and geographic or meteorological factors. Weighting factors include measures such as distance from the predictand location, elevation, station clustering, vertical layer (to account for local inversions), topographic facet (to account for rainshadows), coastal proximity, and effective terrain weights (Daly et al., 2002). We used PRISM estimates for the period 1895-2000, and 1950-1999 as the climatological average period for calculating anomalies. PRISM provides the most topographically precise, methodologically sound, quality controlled historic climate data set available for century-long time scales; thus, PRISM is a robust choice for spatial and topographic concerns that underlie the needs of vegetation modeling.

Global Climate Model (GCM) Projections

We garnered climate model projections, used in the Fourth Assessment Report (AR4) of the Intergovernmental Panel on Climate Change (IPCC), from the Program for Climate Model Diagnosis and Intercomparison (PCMDI) archive. Details on the models and their configurations are available at http://wwwpcmdi. llnl.gov/ipcc/about ipcc.php. These projections used coupled ocean-atmosphere models (AOGCMs) to simulate climate variations spanning the late 19th Century to the end of the 21st century (see Meehl et al., 2007); this generation of models is referred to as Coupled Model Intercomparison Project version 3 (CMIP3). We analyzed, individually, 22 of these models (48 simulations; Table 1) that are forced with estimated greenhouse gas and aerosol changes from the late 19th century through 1999, and the IPCC Special Report on Emissions Scenarios (SRES) A1B

scenario from 2000 to 2100. The A1B scenario, sometimes referred to as "the medium non-mitigation scenario" (Moss et al., 2008), describes a future world of rapid economic growth, with global population that peaks in mid-century then declines, and rapid introduction of new and more efficient technologies that are balanced such that no single source of energy is overly dominant (Nakicenovic et al., 2000). We analyzed total monthly precipitation and monthly mean temperature for each individual model and the 22-model ensemble mean (Hoerling et al., 2007).

Downscaling

The AR4 GCMs use a variety of grid resolutions, typically in the range of approximately 2.5°. (~300 km in middle latitudes) per side of the grid box. The first step in the data treatment is to align the GCMs to a common grid, using inverse distance weighting (Eischeid et al., 2000). Once the GCM estimates for each parameter have been re-gridded, we statistically downscale the GCM estimates to the 4 km grid resolution required for the vegetation change analysis, using the method described by Salathé (2005). To remove the bias between the large-scale simulated climate parameter and the observed climate parameter at each grid cell, we apply monthly corrections so magnitudes of the GCM simulations of the historic period conform to observations for the 1950-1999 period of overlap with the PRISM data. The 20th century runs runs used to fit each model are simulations forced by historic variations in greenhouse gases, solar output, and atmospheric aerosol loading. For each of the models presented here, the 20th century runs were obtained from the PCMDI archive. The aforementioned biases are presumed to be the same from year to year, because at the monthly time scale the models

can resolve the large-scale weather systems that generate observed temperature and precipitation across the Colorado Plateau.

The IPCC Fourth Assessment Report notes that more than 75% of the models overestimated western North America annual and seasonal precipitation (Christensen et al., 2007). The median precipitation bias was highest for winter (93%, December-February) and lowest for summer (28%, June-August); the median annual precipitation biaswas 65%. Western North America temperature was underestimated by most AR4 GCMs (Christensen et al. 2007); the median bias for annual temperature was -1.3°C. The most pronounced underestimation of seasonal temperature was for spring (March-May); the median bias was -2.0°C.

The method uses the PRISM estimates to impose spatial structure to the GCM-simulated precipitation and temperature, while preserving the atmospheric processes driving the simulations. As mentioned by Salathe (2005), Widmann et al. (2003) used a similar method, referred to as "local scaling." The spatial biases and magnitudes are corrected independently for each model, by multiplying the simulated parameters by monthly bias factor (for precipitation) and taking the difference between the simulation and the bias factor (for temperature) at each grid point.

Let $P_{mod}(x, t)$ be the simulated monthly precipitation for the large-scale gridpoint in location x and at time t (in months); $(P_{mod})_{mth}$ is the monthly mean taken over the period

of overlap between the simulated data and observations $(P_{obs})_{mth}$. The downscaled monthly mean precipitation (P_{ds}), then, can be calculated by:

$$P_{ds}(x,t) = P_{mod}(x,t)\,(P_{obs})_{mth}/(P_{mod})_{mth}$$

The fitting is performed independently for each month.

Surface air temperature is downscaled in a similar way. For temperature, the adjustment uses the difference between the mean bias and the observations. Let $T_{mod}(x, t)$ be the simulated monthly temperature, $(T_{mod})_{mth}$ be the simulated monthly mean taken over the fitting period, and $(T_{obs})_{mth}$ be the monthly mean of the observations taken over the fitting period. Then, the downscaled monthly mean surface temperature can be calculated by:

$$T_{ds}(x,t) = T_{mod}(x,t) + [(T_{obs})_{mth} - (T_{mod})_{mth}]$$

This correction assumes that the large-scale temperature predicts the local temperature, given the removal of a monthly bias in the mean. Salathé (2005) notes that this additive methodology may be thought of as a lapse-rate correction due to the elevation difference of the local gridpoint relative to the GCM grid. Like Salathé, we make no allowance for possible changes in the lapse rate as a consequence of climate change. Despite these limitations to the aforementioned methods, and the dependency of this statistical approach on the accuracy of the regional circulation patterns produced by the GCMs (CCSP, 2008a), the method is computationally efficient, and previous studies show a

relatively high confidence in the simulations of storms and jet streams in the middle latitudes (CCSP, 2008a).

Ranking procedure

In order to determine the most appropriate GCMs to use in the vegetation change analyses, we ranked the models, using four metrics based on the fit between the GCM climatological estimates of seasonal precipitation during the period of fit and the observed seasonal precipitation averaged over the period 1950-1999. We compare observed parameters and GCM projections for three seasons chosen for their influence on Colorado Plateau vegetation: November-March (winter), May-June (pre-monsoon) and July-September (monsoon). We did not assess fit between simulated and observed temperature, because it is well known that there is good agreement between model temperature simulations for western North America (IPCC, 2007), and the bias corrections should account for differences in magnitude. We acknowledge that, compared with temperature, spatial variations in precipitation are less well understood and that there is a greater spread between models in simulated precipitation – thus, choice of models can make a difference in the application of projections for decision-making (IPCC 2007; CCSP, 2008a; Brekke et al., 2008). We assume that models that simulate well the recent precipitation history of these key seasons are likely to simulate key characteristics of future climate. In using this metric, we acknowledge that we cannot assess whether well-fitting simulations for our region produce the "right results" for the wrong (mechanistic) reasons.

We computed four values for each model, using metrics computed seasonally and then averaged, for the domain of interest, the continental United States west of 100°W. These are as follows:

- a map pattern relationship based on the correlation coefficient between simulated and observed precipitation, over the domain of interest ;
- a map pattern relationship based on the congruence coefficient for the same;
- the ratio of simulated/observed area-averaged precipitation based on the seasonal precipitation totals in millimeters; and
- the ratio of simulated/observed area averaged precipitation based on the seasonal precipitation expressed as a percentage of the annual total.

These four sets of metrics for each of the 22 models were then ranked, and the ranks summed for each model. The best rank for each metric is 1, and the worst is 22. The best possible cumulative rank is 4, i.e., a rank of 1 for each of the four metrics. For example, the HAD model produced the following ranks: 1, 3, 3, 3, which yielded an overall score of 10 (Table 1).

We acknowledge that the GCMs differ significantly in terms of basic physical and dynamical design and number of atmospheric and oceanic layers; accounting for such factors may have resulted in a different choice of models. For example, process-based measures, such as the ability of a model to reproduce the El Nino-Southern Oscillation (ENSO), are certainly appropriate for studying Colorado Plateau climate; however, a

model with acceptable ENSO simulation may lack acceptable monsoon simulation. Although several studies project decreasing annual precipitation in the southwestern United States (IPCC, 2007; Seager et al., 2007), we recognize the limitations of statistically downscaling GCM output to our study area. As we show below, the annual cycle of precipitation for the western USA is poorly simulated by many of these models. Most GCMs overestimate regional winter precipitation (Christensen et al., 2007).

3. Results: Model selection

The results of the ranking exercise are presented in Table 1. The overall score for the HAD model (10) produced the lowest rank of all models used in this analysis – that is, HAD precipitation for 1950-1999 was most faithful to the seasonal cycle and spatial distribution of precipitation in the observed record. The next closest score was 26 (ECHAM5). For each of the four ranking metrics, the order of models (best/lowest to worst/highest) did not change much (not shown). In other words, any of the above four metrics individually produce the same order as that for summing the four and then ranking the models. Three other models were selected, based on subjective criteria. CSIRO (score 42) and CNRM (score 42), which tied for rank 9 of 19, were included because together they bracket the range of published projections for aridity in the southwestern United States (Seager et al., 2007). Seager and his colleagues modeled precipitation minus evaporation anomalies (P-E) using A1B emissions scenario projections for 19 IPCC AR4 models. Mid-century (2041-2060) projections ranged from

about -0.12 mm/day (CNRM) to no detectable change (with CSIRO and HAD both showing near zero change or slight increases in P-E) (Figure 2 of Seager et al., 2007). NCAR (score 50; rank 11) was selected because of opportunities to use this model in collaboration in collaboration with other investigators, in order to expand further upon this work. None of these five models required flux corrections in order to maintain a stable climate in control runs (Kripalani et al., 2007). A 22-model ensemble mean (22-ME) also was included for comparison with the individual models. Ensemble means generally improve the performance of climate simulations, probably because model errors arise from internal climate variability and uncertainties in model formulation, and such errors effectively cancel out when large numbers of models are averaged (Reichler and Kim, 2008).

Not surprisingly, the GCMs more closely simulate the seasonal cycle of 1950-1999 Colorado Plateau monthly mean temperature than they simulate the seasonal cycle of monthly mean precipitation (Figures 3, 4). This is consistent with results from global-scale studies; Covey et al. (2003) found that historic global temperatures generated by CMIP2 coupled atmosphere-ocean Global Climate Models (AOGCMs) correlated exceedingly well with historic observed temperatures ($r > 0.93$ for each model), whereas correlations between AOGCMs and observed precipitation ranged from 0.4 to 0.7.

Temperature

The ECHAM5 model shows the closest match to the observed seasonal cycle of Colorado Plateau temperatures (Figure 3). HAD exaggerates the seasonal temperature range; HAD

temperatures are too hot in summer and too cold in winter. The NCAR model shows a similar exaggeration of average monthly temperature range. The CNRM and CSIRO models exhibit seasonal cycles similar to the ensemble average: temperatures that are cooler than the observed average during the winter, spring, and fall months, but near the observed average during the summer months.

Because temperature is a more spatially coherent variable, spatial patterns of GCM temperature simulations were less varied those for precipitation (not shown). All models simulate the spatial patterns of observed seasonal temperatures, with variations based primarily on the magnitude of temperature change. In some cases differences between models derive from the spatial resolution of the models, and treatment of topography within the models. For example, the HAD model produces notably cooler than observed November-March temperatures for the northern Rocky Mountains. HAD and NCAR simulated temperatures are warmer than observed during the spring and summer months, throughout most of the West. For November-March temperatures, with the exception of ECHAM5, all models show cooler than observed mean seasonal temperatures for southern New Mexico.

Precipitation

HAD shows the best match with the observed seasonal cycle of precipitation and associated spatial distribution of precipitation (Figure 4). Although HAD predictions for July and August total precipitation are 38.3% and 36.0% higher, respectively, than the observed, it is the only model considered here that does not drastically overestimate

Colorado Plateau winter season precipitation (Figure 4). The NCAR model depicts a Mediterranean climate seasonal cycle of precipitation for the Southern Colorado Plateau (SCP) region, whereas the CSIRO shows little variation in precipitation between months, in contrast to the observed bimodal season cycle. The CNRM, ECHAM5 and the 22-ME all show bimodal seasonal cycles, but overestimate November-March precipitation, as well as April and September precipitation.

Like the 22-ME, most of the individual models considered here overestimate observed November-March precipitation by a factor of two (Table 2). Overestimation of winter precipitation in the U.S. West is a long-standing issue among GCMs (Coquard et al, 2004), related in part to the complex topography of the region (Duffy et al., 2003). Average pre-monsoon arid foresummer season (May-June) precipitation was simulated well by most of the models considered here, with the notable exception of the CSIRO (and the CNRM for May) (Figure 4). The ECHAM5 and CNRM models closely matched the observed June annual precipitation minimum. The CNRM comes closest to simulating the observed monthly means for each summer month, although ECHAM5 total summer precipitation is closest to observed (Table 2). The ECHAM5 and 22-ME underestimate observed July precipitation, and overestimate September precipitation. As mentioned above, the HAD model closely matches the observed seasonal cycle in summer, but it overestimates precipitation in July and August by more than 35% in each month.

Map comparisons of the geographic distribution of precipitation, as depicted by the GCMs and observations, are too numerous to show in this paper; we summarize comparisons for the SCP in Tables 3 and 4. We discuss the most salient aspects for the western U.S. and the SCP, below. In general, the GCMs preserve the spatial structure of seasonal precipitation across the West, showing Mediterranean climates for the coastal states, and monsoon moisture reaching eastern half of the West. Overall, they depict wetter than observed winter precipitation across the West, a somewhat drier than observed spring season across the Rockies and Plains states, and drier than observed summer precipitation, especially in the northern and western parts of the Four Corners states.

For November-March precipitation, the most notable aspects are: NCAR, ECHAM5 and CSIRO depict much wetter than observed conditions throughout the West; the 22-ME and HAD are wetter than observed in the southern Plains; CNRM exaggerates winter wetness in the Southwest and HAD shows drier than observed winter precipitation in the west central Rocky Mountains. Overestimations of November-March precipitation were most obvious in New Mexico, where estimates were more than double the observed precipitation in all five models except HAD, and the northern Plains states. For May-June precipitation, most of the models did not capture the extent of spring moisture in the Plains states, especially in the southern Plains. The CSIRO model depicted a wetter than observed spring in the Southwest (especially New Mexico). For July-September precipitation, the NCAR depicted a western U.S. landscape much drier than observations, which is not surprising, given the Mediterranean seasonal cycle described by the model.

The HAD model depicted realistic spatial structure of Southwest summer precipitation, but underestimated the northern extent of summer precipitation. The CNRM, ECHAM5, CSIRO and 22-ME match the overall spatial structure of summer precipitation in the West, but they all show drier than observed conditions in the Southwest, especially in the western half of the Four Corners states. The 22-ME and CNRM estimate wetter than observed summer precipitation for the Upper Colorado River Basin.

Table 3 presents a qualitative comparison of model estimates versus observed precipitation for the Southern Colorado Plateau (SCP). For November-March, most of the models overestimate SCP mean precipitation. The HAD and 22-ME produce wetter than observed conditions in the southeastern quadrant of the SCP. The CSIRO, ECHAM5, and NCAR models all exhibit wetter than observed winter precipitation, with the ECHAM5 showing more than double the observed precipitation over most of the SCP domain. The CRNM CM3 simulates wetter than observed precipitation over the southern half of the SCP.

For May-June, with the exception of the ECHAM5, all models and the 22-ME produce wetter than observed precipitation in the eastern half of the SCP. In particular, the CSIRO model produces well more than double the observed precipitation in the eastern half of the SCP. For July-September, the differences between models and observations are even more pronounced, with most models showing greater than observed precipitation in the eastern half of the SCP and less than observed precipitation in the western half of the SCP. Similar to the spring season, the CSIRO model produces double the observed

summer precipitation in the eastern half of the SCP; as mentioned above, the CSIRO model does not produce a strong seasonal cycle, and overestimates precipitation in every single month (Figure 4). The NCAR is drier than observed over the entire SCP domain.

4. Results: Model projections for the Southern Colorado Plateau

Projections for the SCP all show increasing temperatures after 1980 (Figure 5). When the 22 model projections are averaged together (22-ME), the temperature increase appears to be nearly monotonic, reaching 2.2°C above the observed average in the 2030s, and 4.0°C above the observed average by the end of the century. Individual models exhibit considerable multi-year variability within the upward trends in temperature. With the exception of the CSIRO model, which projects considerably lower temperature increase of 2.3°C by the end of the century, individual models show increases comparable to the 22-ME. HAD projects the greatest annual temperature increases, reaching 5.4°C above the observed average by 2080.

Seasonal temperature projections (not shown) exhibit slightly higher rates of increase for the arid foresummer and summer seasons than for the cool season. The 22-ME projection for the SCP warm seasons reach 2.5°C above the observed average in the 2030s, and 4.7°C higher than observed average values by the end of the century. November-March seasonal temperature projections reach 1.9°C above the observed average by 2040, and 3.6°C above the average by the end of the century. In all seasons, the CSIRO shows

lower temperature increases than the other models. The HAD projects much higher winter temperature increases than the other models (6.0°C higher than average by the end of the century) and, probably due to its exceedingly high projection of July-September precipitation, less than 22-ME increases during the summer. The NCAR, which characterizes the SCP as having a Mediterranean seasonal precipitation cycle for 1950-1999, projects the greatest summer season temperature increases (4.8°C by the end of the century). Timbal et al. (2008) found the CSIRO the least sensitive (2.11°C) and the ECHAM5 most sensitive (3.69°C) models when comparing the global temperature sensitivity of 10 AR4 GCMs modeling the A1B scenario for the twenty-first century. The HAD was not among the models tested, but similar to this study, CNRM temperature sensitivity was roughly in the middle (2.81°C).

SCP precipitation projections show a wide range of possibilities, and few coherent trends. This is not surprising, and is consistent with the CCSP (2008a) and IPCC (2007) statements that AOGCMs are often not reliable for simulating sub-continental scale precipitation. The 22-ME projection suggests a slight decline (6.5%) in annual precipitation for the Colorado Plateau (Figure 6). Most of the GCMs we selected project annual precipitation below the observed 1950-1999 average for most of the 21st Century. Most models show decade-scale variations, with few pluvials of the magnitude seen during the 20th Century. HAD, however, projects higher than observed mean SCP precipitation for most of the 21st Century, due to several decade-scale winter pluvials, and an overall increase in summer precipitation, averaging 50% above observed, after 2040 (Figures 6-9). SCP November-March precipitation projections indicate great variability

between models and no strong trends (Figure 7); the 22-ME projects a slight decline in winter precipitation of about 5% during the course of the century.

SCP May-June precipitation projections agree on mostly below observed average precipitation during the course of the 21st Century, with some substantial differences in multi-decade variability and the magnitude of declining arid foresummer precipitation (Figure 8). In particular, the 22-ME declines throughout the century, averaging about 75% of climatology during the last decades of the century. The CNRM projects the greatest decline in SCP May-June precipitation (47.8%, with an average of 50% lower than climatology for the last 3 decades of the century). The CSIRO projects consistently below average SCP May-June precipitation, reaching about 25% below climatology by the last few decades of the century (Figure 8). Though a small fraction of annual precipitation falls during the arid foresummer, temperatures during this time of year may be implicated in massive forest mortality (Breshears et al., 2005; Weiss et al., 2009 [in press]).

SCP July-September precipitation projections also indicate great variability between models and no clear trends; the 22-ME projects a slight increase in summer precipitation during the course of the century, modulated by multi-decadal variability (Figure 9). The HAD model shows a clear and dramatic increase in SCP summer precipitation after 2020, with regional totals far in excess of observations. On the other hand, the ECHAM5 model projects mostly below observed average SCP summer precipitation during the 21st century. Summer season precipitation in the western U.S. is notoriously difficult to

predict. The IPCC (2007) indicates relatively low agreement for the SCP between 21 GCMs used to project summer (June-August) precipitation in the West. A study by Lin et al. (2008) determined that most of the AR4 models overestimate precipitation in the core monsoon region and fail to show the monsoon retreat.

In this study, the two top-ranking GCMs, based on their skill in simulating observed average precipitation in the West (Table 1), project radically different precipitation changes in the mid-century example considered; this is particularly the case for summer precipitation (Figure 10; Table 4). For mid-century July-September precipitation, the HAD projects a 30% increase for the Colorado Plateau area, whereas the ECHAM5 projects a comparable decrease for the western three-fourths of the domain (Table 4). For May-June mid-century precipitation (Table 4), the two models show greater agreement with each other, with prominent drying in the western two-thirds of the domain. The two models project a slight increase in May-June precipitation for the eastern part of the SCP domain, in contrast to the 22-ME projection. For November-March mid-century projections, similarly, the two models show a slight increase in precipitation for much of the SCP, while the 22-model ensemble projects a slight decrease in the southern half of the SCP (Figure 11; Table 4).

5. Discussion

Model Selection and Vegetation Modeling

The fact that two GCMs included in this study captured the global extremes of temperature sensitivity as tested by Timbal et al. (2008) suggests that our model selection process succeeded in bracketing a range of temperature increases, which is important for modeling potential changes in vegetation distribution. In all seasonal precipitation projections, the ensemble projection falls about midway between the projections by the selected models, suggesting the five selected models are showing similar variability as the full set of 22 models. (N.B.: Results from a separate analysis, using the ensemble mean of the 5 highest ranking models [Table 1], do not differ dramatically from the major findings of the analysis presented herein). As with temperature sensitivity, the selected models span the full range of precipitation projections, which suits the goal of the selection process in capturing the range of possibilities for bracketing potential vegetation responses.

Work by Seager et al. (2007) further indicates that the model selection process captured a substantial range of projections. Considering the Southwest quadrant of the United States, Seager and his colleagues modeled precipitation minus evaporation (P-E) using A1B emissions scenarios for 19 IPCC AR4 model projections. Mid-century (2041-2060) projections ranged from about -0.12 mm/day (CNRM) to no detectable change (CSIRO and HAD; Figure 2 of Seager et al., 2007). Overall, these results revealed a much more consistent projection for increased aridity than would be suggested by the precipitation projections alone, because models consistently projected increases in temperature. Although this study did not combine temperature and precipitation into an aridity value, vegetation modeling will integrate these two factors. The combination of increasing

temperatures without a substantial concomitant increase in precipitation affects P-E, which impacts soil moisture and vegetation dynamics (e.g., Breshears et al., 2005; Adams et al., 2009, Weiss et al., 2009 [in press]).

Of the models selected for this analysis, the HAD presents some of the most intriguing possibilities for modeling future vegetation distribution. HAD ranked highest in closeness to observed precipitation seasonal cycle and spatial variation of precipitation (Table 1); however, HAD shows markedly warmer than observed summer temperatures and markedly cooler than observed winter temperatures. HAD A1B scenario projections for the SCP tend toward warmer and wetter in the winter season (Figure 4) and (relatively) cooler and wetter during the summer. Given the recent emphasis on drought, these scenarios have not been addressed much in the recent climate-vegetation analysis literature for the southwestern U.S. Paleoclimate and paleoecological studies may shed light on expectations for the kinds of changes projected by the HAD model.

Implications for Climate Processes and Ecosystem Impacts

Based on the results described above, the Southern Colorado Plateau annual temperatures are projected to increase by 1.5°-3.6°C by mid-century (22-ME = 2.9°C), and by 2.53°-5.4°C by the end of the century (22-ME = 4.0°C), with annual temperatures exceeding the 1950-1999 range of variability by the 2030s. Annual precipitation changes are less clear. A conservative estimate, using a 22 model ensemble average, indicates that SCP annual precipitation may decrease by 6% by the end of the century. The clearest indication is that SCP May-June arid foresummer precipitation is likely to decline, by 11-

45% (conservatively, 25%). The majority of 21st century precipitation variations do not consistently exceed the range of historic variability.

The aforementioned results are consistent with IPCC AR4 projections, and with studies that have examined projections for northern California (Dettinger, 2006) and the Upper Colorado River Basin (Christensen and Lettenmaier, 2007). The hydroclimatic implications of increasing temperatures coupled with precipitation variability dominated by interannual and decadal change, but lacking trend, are well known. These include decreasing snowpack (Mote et al., 2005; Rauscher et al., 2008), early snowmelt (Stewart et al., 2004; 2005; 2009), and an increased fraction of liquid winter precipitation (Knowles et al., 2006), decreased runoff (Milly et al., 2005; Ellis et al., 2008), and increased evapotranspiration (Hamlet et al., 2007).

The downscaling approach used in this study does not preserve within-month variability; consequently, ephemeral events such as flood-producing intense rains, frosts, extreme daily temperatures, and wilt-inducing hot, dry episodes are not captured. Studies by Diffenbaugh et al. (2005), using regional climate models, and Meehl et al. (2004) show that projected increases in mean temperature across North America are associated with the aforementioned phenomena – all of which have strong effects on vegetation. In particular, temperature-limited growth processes and the combination of increased temperatures and soil moisture deficits can affect widespread tree mortality and treeline conifer species distribution (e.g., Adams et al., 2009; van Mantgem et al., 2009; Schrag et al., 2008). Moreover, Weiss et al. (2009 [in press]) demonstrate that increased late spring

temperatures and drying, consistent facets of the projections used in this study, increase evapotranspirational demand and vegetation moisture stress.

Yet, climate and ecological correlates of climate do not completely predict the present ranges and distributions of vegetation. Extreme climatic events, insects, diseases, soil processes, and large scale disturbance processes, such as fire, are examples of ecological limiters contributing to species mortality, recruitment, and distributions (Swetnam and Betancourt, 1998). Climate variability is dampened in the ensemble mean results, so the use of individual model projections allows a more realistic simulation of annual and multidecadal climate fluctuations for vegetation modeling. Variability influences many ecological processes that can affect species distribution, including seedling germination and survival, herbivore pressure, pollinator phenology, and wildfire frequency and extent. For example, dry wildfire seasons that follow relatively wet years can be associated with more area-burned than dry seasons following dry years in some cases (Swetnam and Betancourt, 1998). The next step we need to take in our modeling efforts is to incorporate key ecological limiters with climate limiters to provide more realistic species responses.

6. Conclusions

In this study, we statistically downscaled selected IPCC AR4 GCMs for the western United States. Our statistical downscaling method rapidly, and at little cost, provided simulations of future climate at a spatial scale acceptable for vegetation modeling.

Models were selected for their simulation of Southern Colorado Plateau climate, and for characteristics that would produce a range of future climatic conditions to drive vegetation change simulation models. Our evaluation of models, based on their simulation of the seasonal cycle of precipitation and spatial correlation between GCMs and observed precipitation, revealed that all models overestimate annual SCP precipitation, and that few models match the observed SCP seasonal cycle of precipitation. Models better estimated the seasonal cycle of SCP temperatures, but several models exhibited biases toward warmer than observed summer temperatures and cooler than observed winter temperatures. The HAD model displayed the closest match with historic precipitation observations, but some of the projections from HAD are beyond the edge of the envelope of projections of other models. Perhaps most important is that our analysis demonstrated that the models selected for vegetation analysis produce substantially greater variability than ensembles (an obvious result) and, in this case, a rich array of variability and potential future climates.

The aforementioned biases in GCMs make choosing a "best model" based only on comparison with historic temperature and precipitation a dubious process. Even using a more comprehensive set of metrics can mute the differences between ensembles of models, and can, for a specific region, produce the correct answers for the wrong reasons (Brekke et al., 2008). Yet, using ensemble mean simulations removes the vulnerability needed for realistic vegetation change modeling. One prospect for future research is to use regional climate model simulations that dynamically downscale GCM projections to finer spatial scales.

Projections of future temperature and precipitation, based on individual models and a 22-model ensemble mean, show excellent agreement with regard to SCP temperature increases; however, differences in magnitude between GCMs spanned more than 3°C in each season, and for annual temperature. For future precipitation, the most important result is that the selected models show a strong downward trend in May-June precipitation; in combination with increasing temperatures, lack of moisture during this time of year could increase the likelihood of massive forest mortality events, such as the die-off of Colorado Plateau conifers in the early part of the 21st century.

Acknowledgments. This work was funded by Department of Energy National Institute for Climate Change Research, project MPC35TV-02, "Regional Dynamic Vegetation Model for the Colorado Plateau: a Species-Specific Approach." The authors acknowledge Dr. Andrew Ellis, Arizona State University, for providing estimated potential evapotranspiration data for the Colorado Plateau region. The authors also acknowledge the communications and design staff of the University of Arizona Institute of the Environment for assistance with graphics.

References

Adams, H. D., M. Guardiola-Claramonte, G. A. Barron-Gafford, J. Camilo Villegas, D. D. Breshears, C. B. Zou, P. A. Troch, and T. E. Huxman, 2009. Temperature sensitivity of drought-induced tree mortality portends increased regional die-off under global-change-type drought. Proceedings of the National Academy of Sciences 106(17): 7063-7066. DOI: 10.1073/pnas.0901438106

Bachelet, D., R.P. Neilson, T. Hickler, R.J. Drapek, J.M. Lenihan, M.T. Sykes, B. Smith, S. Sitch, K. Thonicke. 2003. Simulating past and future dynamics of natural ecosystems in the United States. Global Biogeochemical Cycles 17(2):14-1 - 14-21.

Bonan G. B., Levis S., Sitch S., Vertenstein M., Oleson K.W. 2003. A dynamic global vegetation model for use with climate models: concepts and description of simulated vegetation dynamics. *Global Change Biology* 9: 1543–1566.

Brekke, L. D., Dettinger, M. D., Maurer, E. P., and Anderson, M.: Significance of model credibility in estimating climate projection distributions for regional hydroclimatological risk assessments, Clim. Change, 89, 371–394, doi: 10.1007/s10584-007-9388-3.

Breshears, D. D., N. S. Cobb, P. M. Rich, K. P. Price, C. D. Allen, R. G. Balice, W. H. Romme, J. H. Kastens, M. L. Floyd, J. Belnap, J. J. Anderson, O. B. Myers, and C. W. Meyer. *2005.* Regional vegetation die-off in response to global-change-style drought. Proceedings of the National Academy of Sciences 102(42): 15144-8.

Burkett, V.R., D.A. Wilcox, R. Stottlemyer, W. Barrow, D. Fagre, J. Baron, J. Price, J.L. Nielsen, C.D. Allen, D.L. Peterson, G. Ruggerone, and T. Doyle. 2005. Nonlinear dynamics in ecosystem response to climatic change: case studies and policy implications. Ecological Complexity 2: 357-3.

Cayan, D. R., S. A. Kammerdiener, et al., 2001. Changes in the Onset of Spring in the Western United States. Bulletin of the American Meteorological Society: 399-415.

CCSP, 2008a: *Climate Models: An Assessment of Strengths and Limitations.* A Report by the U.S. Climate Change Science Program and the Subcommittee on Global Change Research [Bader, D.C., C Covey, W.J. Gutowski, I.M. Held, K.E. Kunkel, R.L. Miller, R.T. Tokmakian and M.H. Zhang (Authors)]. Department of Energy, Office of Biological and Environmental Research, Washington, D.C., 124 pp.

CCSP, 2008b: *Weather and Climate Extremes in a Changing Climate*. Regions of Focus: North America, Hawaii, Caribbean, and U.S. Pacific Islands. A Report by the U.S. Climate Change Science Program and the Subcommittee on Global Change Research. [Thomas R. Karl, Gerald A. Meehl, Christopher D. Miller, Susan J. Hassol, Anne M. Waple, and William L. Murray (eds.)]. Department of Commerce, NOAA's National Climatic Data Center, Washington, D.C., USA, 164 pp.

Christensen, J.H., B. Hewitson, A. Busuioc, A. Chen, X. Gao, I. Held, R. Jones, R.K. Kolli, W.-T. Kwon, R. Laprise, V. Magaña Rueda, L. Mearns, C.G. Menéndez, J. Räisänen, A. Rinke, A. Sarr and P. Whetton, 2007: Regional Climate Projections.

In: *Climate Change 2007: The Physical Science Basis. Contribution of Working Group I to the Fourth Assessment Report of the Intergovernmental Panel on Climate Change* [Solomon, S., D. Qin, M. Manning, Z. Chen, M. Marquis, K.B. Averyt, M. Tignor and H.L. Miller (eds.)]. Cambridge University Press, Cambridge, United Kingdom and New York, NY, USA.

Christensen, N. and D. P. Lettenmaier, 2007. A multimodel ensemble approach to assessment of climate change impacts on the hydrology and water resources of the Colorado River basin. *Hydrology and Earth System Sciences Discussions* 11(1417-1434).

Coquard, J., P. B. Duffy, K. E. Taylor, and J. P. Iorio, 2004. Present and future climate in the western USA as simulated by 15 global climate models. Climate Dynamics 23: 455-472.

Daly, C., R.P. Neilson, and D.L. Phillips. 1994. A statistical-topographic model for mapping climatological precipitation over mountainous terrain. *Journal of Applied Meteorology* 33: 140-158.

Daly, C., G.H. Taylor, W. P. Gibson, T.W. Parzybok, G. L. Johnson, P. Pasteris. 2001. High-quality spatial climate data sets for the United States and beyond. *Transactions of the American Society of Agricultural Engineers 43: 1957-1962.*

Daly, C., W. P. Gibson, G.H. Taylor, G. L. Johnson, P. Pasteris. 2002. A knowledge-based approach to the statistical mapping of climate. *Climate Research*, 22: 99-113.

Dettinger, M. D., 2005. From climate change spaghetti to climate change distributions for 21st century. San Francisco Estuary Watershed Science 3(1):1–14.

Diffenbaugh, N. S., J. S. Pal, et al., 2005. Fine-scale Processes Regulate the Response of Extreme Events to Global Climate Change. *Proceedings of the National Academy of Sciences* 102(44): 15774-8.

Eischeid JK, Pasteris PA, Diaz HF, Plantico MS, Lott NJ. 2000. Creating a serially complete, national daily time series of temperature and precipitation for the western United States. *Journal of Applied Meteorology* **39**: 1580-1591.

Ellis, A.W., T.W. Hawkins, R.C. Balling and P. Gober. 2008. Estimating future runoff levels for a semiarid fluvial system in central Arizona. *Climate Research* 35:227-239.

Hamon, W.R., 1961. Estimating potential evapotranspiration. *Proceedings of the American Society of Civil Engineering* 871: 107-120.

Higgins, R. W., Y. Chen, and A. V. Douglas, 1999. Interannual variability of the North American warm season precipitation regime. *J. Climate,* **12,** 653–680.

Hoerling, M., J Eischeid, X Quan, T Xu, 2007. Explaining the record US warmth of 2006. Geophysical Research Letters, 34, L17704, doi:10.1029/2007GL030643.

IPCC, 2007: Climate Change 2007: The Physical Science Basis. Contribution of Working Group I to the Fourth Assessment Report of the Intergovernmental Panel on Climate Change [Solomon, S., D. Qin, M. Manning, Z. Chen, M. Marquis, K.B. Averyt, M. Tignor and H.L. Miller (eds.)]. Cambridge University Press, Cambridge, United Kingdom and New York, NY, USA, 996 pp.

Jackson S. T. and J. T. Overpeck, 2000. Responses of plant populations and communities to environmental changes of the late Quaternary. *Paleobiology* 26:194–220.

Knowles, N., M.D. Dettinger, and D.R. Cayan, 2006. Trends in Snowfall versus Rainfall in the Western United States. *Journal of Climate*, **19**(18), 4545-4559.

Kripalani, R.H., J.H. Oh, H.S. Chaudhari, 2007. Response of the East Asian summer monsoon to doubled atmospheric CO_2: Coupled climate model simulations and projections under IPCC AR4. Theoretical and Applied Climatology 87: 1-28.

Lin, J.-L., B.E. Mapes, K.M. Weickmann, G.N. Kiladis, S.D. Schubert, M.J. Suarez, J.T. Bacmeister, and M.-I. Lee, 2008. North American monsoon and convectively coupled equatorial waves simulated by IPCC AR4 coupled GCMs. Journal of Climate 21(12):2919-2937. DOI:10.1175/2007JCLI1815.1.

Logan, J. A., J. Régnière, and J. A. Powell. 2003. Assessing the impacts of global climate change on forest pests. Frontiers in Ecology and the Environment 1: 130-137

Meehl G.A., C. Covey, T. Delworth, M. Latif, B. McAvaney, J.F.B. Mitchell, R.J. Stouffer and K.E. Taylor, 2007: THE WCRP CMIP3 Multimodel Dataset: A New Era in Climate Change Research, *BAMS*, **88**, 1383-1394, DOI: 10.1175/BAMS-88-9-1383

Meehl, G.A., C. Tebaldi and D. Nychka, 2004: Changes in frost days in simulations of twentyfirst century climate *Climate Dynamics* 23: 495–511

Milly, P. C. D., K. A. Dunne, et al., 2005. Global pattern of trends in streamflow and water availability in a changing climate. *Nature* 438: 347-350.

Morin, X., et al., 2008. Tree species range shifts at a continental scale: new predictive insights from a process-based model. *J. Ecol*. **96**: 784–794.

Moss, R. M. Babiker, S. Brinkman, E. Calvo, T. Carter, J. Edmonds, I. Elgizouli, S. Emori, L. Erda, K. Hibbard, R. Jones, M. Kainuma, J. Kelleher, J. Francois Lamarque, M. Manning, B. Matthews, J. Meehl, L. Meyer, J. Mitchell, N. Nakicenovic, B. O'Neill, R. Pichs, K. Riahi, S. Rose, P. Runci, R. Stouffer, D. van Vuuren, J. Weyant, T. Wilbanks, J. Pascal van Ypersele, and M. Zurek, 2008. *Towards New Scenarios for Analysis of Emissions, Climate Change, Impacts, and Response Strategies*. Intergovernmental Panel on Climate Change, Geneva, 132 pp.

Mote, P. W., A. F. Hamlet, M. P. Clark, and D. P. Lettenmaier, 2005. Declining mountain snowpack in western North America. *Bull. Amer. Meteor. Soc.*, **86,** 39–49.

Nakicenovic, N. et al (2000). *Special Report on Emissions Scenarios: A Special Report of Working Group III of the Intergovernmental Panel on Climate Change*, Cambridge University Press, Cambridge, U.K., 599 pp. Available online at: http://www.grida.no/climate/ipcc/emission/index.htm

Rauscher, S. A., J. S. Pal, N. S. Diffenbaugh, and M. M. Benedetti, 2008. Future changes in snowmelt-driven runoff timing over the western US. Geophysical Research Letters, 35, L16703, doi:10.1029/2008GL034424.

Rehfeldt, G. E., Crookston, N. L., Warwell, M. V. & Evans, J. S., 2006. Empirical analyses of plant–climate relationships for the western United States. *International Journal of Plant Sciences*, **167**, 1123–1150

Salathé, E.P. 2005. Downscaling simulations of future global climate with application to hydrologic modelling. *International Journal of Climatology* 25:419-436.

Savage, M., Brown, P.M., and Feddema, J. 1996. The role of climate in a pine forest regeneration pulse in the southwestern United States. Ecoscience 3: 310–318.

Schrag, A. M., A. G. Bunn, and L. J. Graumlich, 2008. Influence of bioclimatic variables on tree-line conifer distribution in the Greater Yellowstone Ecosystem: implications for species of conservation concern. Journal of Biogeography 35(4): 698-710. DOI: 10.1111/j.1365-2699.2007.01815.x

Seager R, Ting M, Held I, Kushnir Y, Lu J, Vecchi G., 2007. Model Projections of an Imminent Transition to a More Arid Climate in Southwestern North America. Science 316(5828): 1181-1184.

Shaw, J. D., Steed, B. E.; DeBlander, L. T. 2005. Forest Inventory and Analysis (FIA) annual inventory answers the question: What is happening to pinyon-juniper woodlands? Journal of Forestry 103(6): 280-285.

Stephenson, N., D. Peterson, D. Fagre, C. Allen, D. McKenzie, and J. Baron. 2006. Response of western mountain ecosystems to climatic variability and change: the Western Mountain Initiative. Park Science. 34 (1): 24-29 p.

Stewart, I. T., D. R. Cayan, et al., 2004. Changes in snowmelt runoff timing in western North American under a 'business as usual' climate change scenario. Climatic Change 62: 217-32.

Stewart, I. T., D. R. Cayan, et al., 2005. Changes toward Earlier Streamflow Timing across Western North America. Journal of Climate 18: 1136-55.

Stewart, I. T., 2009. Changes in snowpack and snowmelt runoff for key mountain regions. Hydrological Processes 23(1): 78-94. DOI: 10.1002/hyp.7128

Stockwell, D.R.B., 2006. Improving ecological niche modeling by data mining large environmental datasets for surrogate models. Ecological Modelling 192: 188-196.

Swetnam, T.W., and J.L. Betancourt, 1998. Mesoscale disturbance and ecological response to decadal climatic variability in the American Southwest. Journal of Climate 11: 3128-3147.

Thompson, R. S., S. E. Hostetler, P. J. Bartlein, and K. H. Anderson, 1998. A strategy for assessing potential future changes in climate, hydrology, and vegetation in the western United States. USGS Circular 1153. (http://pubs.usgs.gov/circ/1998/c1153/c1153_4.htm)

Timbal, B., P. Hope, and S. Charles, 2008. Evaluating the consistency between statistically downscaled and global dynamical model climate change projections. *Journal of Climate* 21: 6052-6059.

USDA Forest Service Southwest Region, aerial survey results posted at http://www.fs.fed.us/r3/resources/health/beetle/index.shtml . Last accessed on Dec. 18, 2008.

van Mantgem P.J., et al., 2009. Widespread increase of tree mortality rates in the western United States. *Science* 323:521–524. DOI: 10.1126/science.1165000

Weiss, J.L., C.L. Castro, and J.T. Overpeck, in review. Distinguishing pronounced droughts in the Southwestern U.S.A.: Seasonality and Effects of Warmer Temperatures. *Journal of Climate*. [Revised version sent 18 March 2009]

Westerling, A. L., Hidalgo, H.G., Cayan, D.R., Swetnam, T.W., 2006. Warming and Earlier Spring Increase Western U.S. Forest Wildfire Activity. Science 313(5789): 940-943.

Figure Captions

Figure 1. Western United States and Southern Colorado Plateau (shaded box) domains used in this study.

Figure 2. Southern Colorado Plateau moisture balance. (A) Mean monthly temperature, precipitation, and potential evapotranspiration (PE) for 1950-1999. (B) Precipitation minus potential evapotranspiration. Potential evapotranspiration is calculated using Hamon's method (Hamon, 1961). Data: PRISM 4 km (Daly et al., 1994); PE calculations provided by Andrew Ellis, Arizona State University.

Figure 3. Southern Colorado Plateau observed (bars) and GCM simulated (lines) mean monthly temperature (°C), 1950-1999. See Table 1 for GCM acronyms. "Ens Avg" refers to the ensemble mean of 22 GCMs used in the IPCC Fourth Assessment Report data set (Meehl et al., 2007). Observed data: PRISM 4 km (Daly et al., 1994).

Figure 4. Southern Colorado Plateau observed (bars) and GCM simulated (lines) mean monthly precipitation (mm), 1950-1999. See Table 1 for GCM acronyms. "Ens Avg" refers to the ensemble mean of 22 GCMs used in the IPCC Fourth Assessment Report data set (Meehl et al., 2007). Observed data: PRISM 4 km (Daly et al., 1994).

Figure 5. Southern Colorado Plateau observed (shaded) and GCM projected (lines) mean annual temperature (°C). See Table 1 for GCM acronyms. "22-mdl Ensemble" refers to the ensemble mean of 22 GCMs used in the IPCC Fourth Assessment Report data set (Meehl et al., 2007). Observed data: PRISM 4 km (Daly et al., 1994).

Figure 6. Southern Colorado Plateau observed (shaded) and GCM projected (lines) mean annual precipitation (mm). See Table 1 for GCM acronyms. "22-mdl Ensemble" refers to the ensemble mean of 22 GCMs used in the IPCC Fourth Assessment Report data set (Meehl et al., 2007). Observed data: PRISM 4 km (Daly et al., 1994).

Figure 7. Southern Colorado Plateau observed (shaded) and GCM projected (lines) mean November-March total precipitation (mm). See Table 1 for GCM acronyms. "22-mdl Ensemble" refers to the ensemble mean of 22 GCMs used in the IPCC Fourth Assessment Report data set (Meehl et al., 2007). Observed data: PRISM 4 km (Daly et al., 1994).

Figure 8. Southern Colorado Plateau observed (shaded) and GCM projected (lines) mean May-June total precipitation (mm). See Table 1 for GCM acronyms. "22-mdl Ensemble" refers to the ensemble mean of 22 GCMs used in the IPCC Fourth Assessment Report data set (Meehl et al., 2007). Observed data: PRISM 4 km (Daly et al., 1994).

Figure 9. Southern Colorado Plateau observed (shaded) and GCM projected (lines) mean July-September total precipitation (mm). See Table 1 for GCM acronyms. "22-mdl Ensemble" refers to the ensemble mean of 22 GCMs used in the IPCC Fourth

Assessment Report data set (Meehl et al., 2007). Observed data: PRISM 4 km (Daly et al., 1994).

Figure 10. Southern Colorado Plateau GCM projected mean July-September total precipitation (mm), 2050. Left: HAD; Center: ECHAM; Right: 22-Model ensemble. See Table 1 for GCM acronyms. Heavy black lines separate above and below 1950-1999 mean; A = Above; B = Below.

Figure 11. Southern Colorado Plateau GCM projected mean July-September total precipitation (mm), 2050. Left: HAD; Center: ECHAM; Right: 22-Model ensemble. See Table 1 for GCM acronyms. Heavy black lines separate above and below 1950-1999 mean; A = Above; B = Below.

Table 1. GCM rankings for spatial correlation between GCM simulation and observed seasonal precipitation over land in the western United States, 1950-1999. Low rank indicates the best combined correlations with the annual cycle of precipitation. **Bold** font indicates GCM identifiers used in the text.

GCM	Modeling Center, Country	Rank
HAD*GEM1*	Hadley Centre, UK	10
ECHAM5*/MPI*	Max Planck Institute, Germany	26
ECHAM4/MPI	Max Planck Institute, Germany	27
CGCM3.1/T63	Canadian Centre for Climate Modelling & Analysis	29
GFDL-CM2.1	NOAA Geophysical Fluid Dynamics Lab, US	35
CGCM3.1/T47	Canadian Centre for Climate Modelling & Analysis	37
GISS-EH	NASA Goddard Institute for Space Studies, US	37
HadCM3-UKMO	Hadley Centre, UK	38
MIROC3.2(medres)	Center for Climate System Research (The University of Tokyo), National Institute for Environmental Studies, and Frontier Research Center for Global Change (JAMSTEC), Japan	39
CNRM CM3	Météo-France / Centre National de Recherches Météorologiques, France	42
CSIRO MK3.0	CSIRO, Australia	42
MIROC 3.2(hires)	Center for Climate System Research (The University of Tokyo), National Institute for Environmental Studies, and Frontier Research Center for Global Change (JAMSTEC), Japan	44
MIUB ECHO-G	Meteorological Institute of the University of Bonn, Meteorological Research Institute of KMA, and Model and Data group.	50
NCAR CCSM3	National Center for Atmospheric Research, US	50
GISS-ER	NASA Goddard Institute for Space Studies, US	53
NCAR PCM1.0	National Center for Atmospheric Research, US	56
BCCR BCM2.0	Bjerknes Centre for Climate Research, Norway	58
GFDL-CM2.0	NOAA Geophysical Fluid Dynamics Lab, US	62
GISS-AOM	NASA Goddard Institute for Space Studies, US	63
IAP-FGOALS	Institute of Atmospheric Physics, People's Republc of China	67
ISPL-CM4	Institut Pierre Simon Laplace, France	71
INM-CM3.0	Institute for Numerical Mathematics, Russia	76

Table 2. Observed and simulated temperature (top) and precipitation (bottom) for the three seasons analyzed in this study (November-March; May-June; July-September). See Table 1 for GCM acronyms. "22-ME" refers to the ensemble mean of 22 GCMs used in the IPCC Fourth Assessment Report data set (Meehl et al., 2007). Observed data: PRISM 4 km (Daly et al., 1994). Temperature is in °C. Precipitation is in mm.

TEM	PRISM	CNRM	ECHAM5	NCAR	CSIRO	HAD	22-ME
NOV-MAR	2.0	-0.3	1.8	-0.7	-0.5	-1.0	-0.3
MAY-JUN	16.6	16.0	17.2	20.0	16.2	21.1	17.9
JUL-SEP	20.4	21.5	21.2	23.9	20.7	24.6	22.1
PRECIP	**PRISM**	**CNRM**	**ECHAM5**	**NCAR**	**CSIRO**	**HAD**	**22-ME**
NOV-MAR	131.5	197.9	306.2	285.5	267.3	128.8	263.4
MAY-JUN	27.9	50.7	31.3	40.8	99.8	50.2	63.4
JUL-SEP	108.5	123.8	107.3	45.2	156.8	138.4	103.6

Table 3. Qualitative assessment of GCM simulated precipitation compared to observations (1950-1999) for the Southern Colorado Plateau (SCP; see Figure 1). Each bold outlined box represents the SCP, and each quadrant of a bold outlined box represents one quadrant of the domain, corresponding to Figure 1 (clockwise from left, NW NE, SE, SW). Sign indicates the direction of projection, boldness indicates magnitude. **+** much greater than observed; + greater than observed; – less than observed; **—** much less than observed. Blanks indicate approximately similar total precipitation.

Model	Winter PPT (Nov-Mar)		Spring PPT (May-Jun)		Summer PPT (Jul-Sep)	
22-Model Ensemble			+	**+**	–	+
		+		+	–	+
UKMO-HADGEM1				+	–	+
		+		+	–	+
MPI-ECHAM5	**+**				–	+
	+	**+**			–	+
CSIRO-MK3	+	+	+	**+**		**+**
	+	**+**	+	**+**	–	**+**
CNRM-CM3				+	–	+
	+	**+**		+	–	**+**
NCAR-CCSM3	**+**	+		+	–	–
	+	**+**		+	**—**	–

Table 4. Qualitative assessment of precipitation projections for mid-century (2050) are compared to observations (1950-1999) for the Southern Colorado Plateau (SCP; see Figure 1). Each bold outlined box represents the SCP, and each quadrant of a bold outlined box represents one quadrant of the domain, corresponding to Figure 1 (clockwise from left, NW NE, SE, SW). Sign indicates the direction of projection; boldness indicates the magnitude of the projection. **+** large increase; + increase; – decrease; **—** large decrease.

Model	Winter PPT (Nov-Mar)		Spring PPT (May-Jun)		Summer PPT (Jul-Sep)	
22-Model Ensemble	+	+	—	–	+	+
	–	–	—	–	+	+
UKMO-HADGEM1	+	+	–	–	**+**	**+**
	+	–	–	–	**+**	**+**
MPI-ECHAM5	+	+	–	–	—	–
	–	–	—	–	—	–
CSIRO-MK3	+	+	–	–	–	–
	+	+	—	–	–	–
CNRM-CM3	–	–	—	—	+	–
	–	–	—	—	+	–
NCAR-CCSM3	–	–	—	–	**+**	+
	–	–	–	–	**+**	+

Figure 1

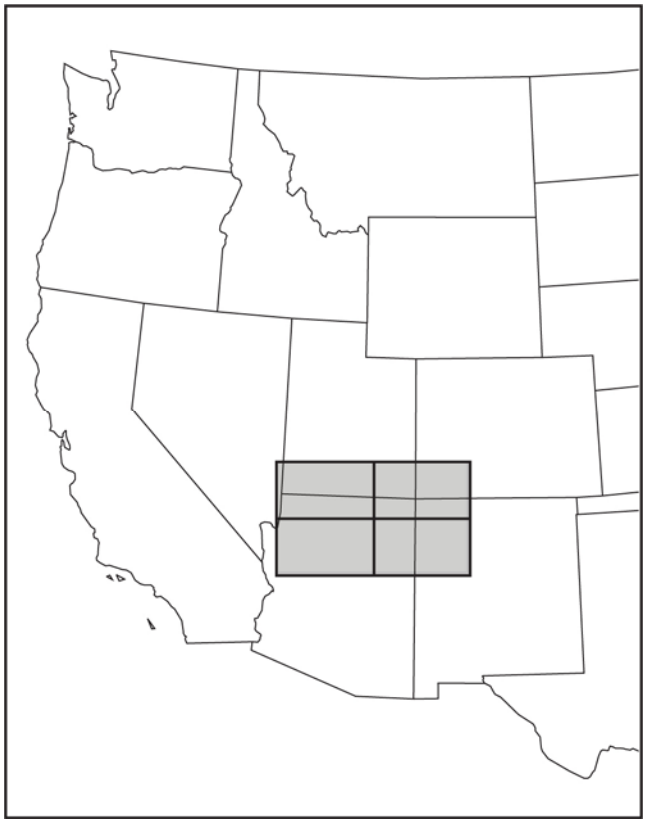

Figure 2

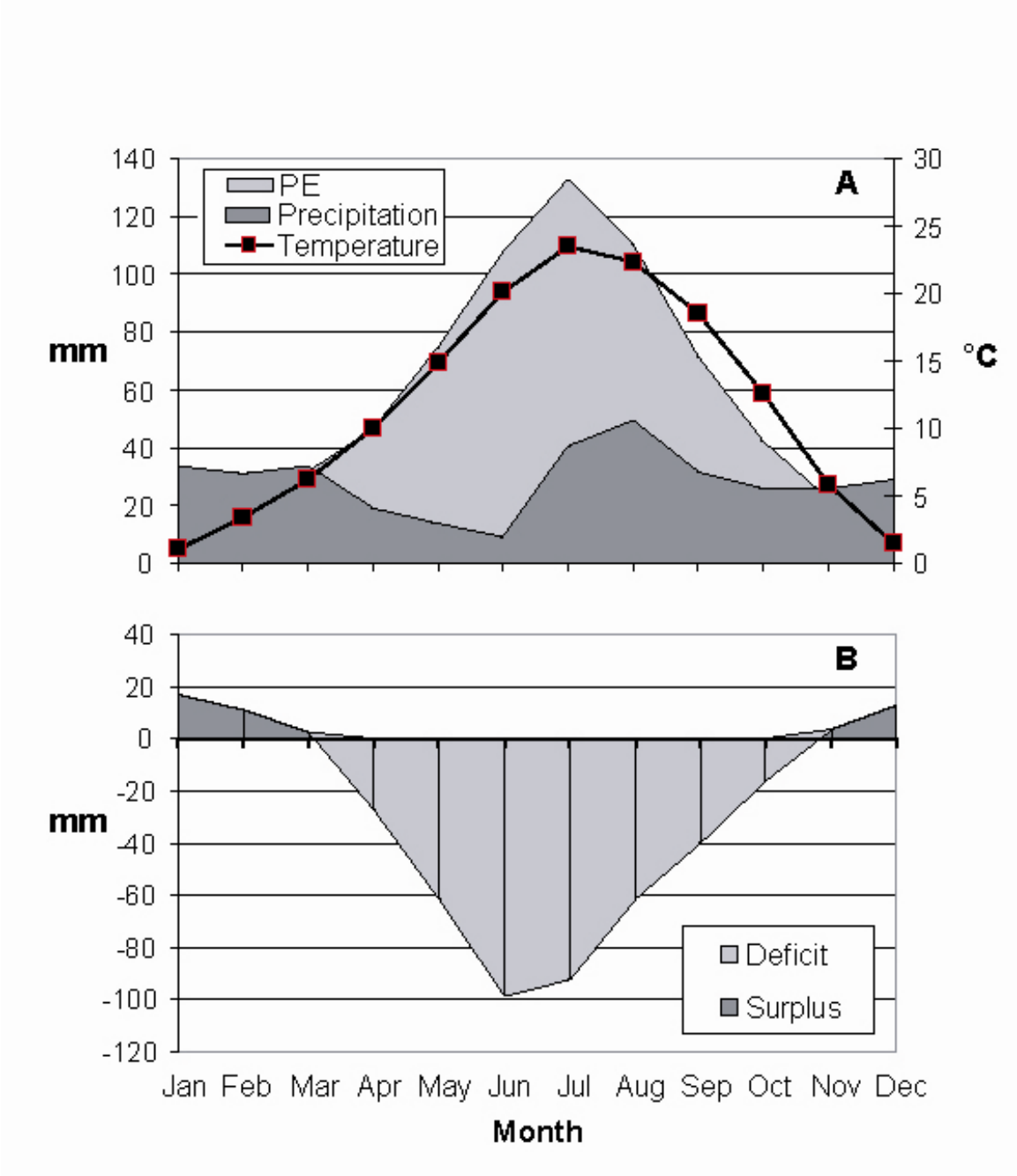
PE
Precipitation
Temperature
A
mm
°C
140
120
100
80
60
40
20
0
30
25
20
15
10
5
0
B
mm
40
20
0
-20
-40
-60
-80
-100
-120
Deficit
Surplus
Jan Feb Mar Apr May Jun Jul Aug Sep Oct Nov Dec
Month

Figure 3

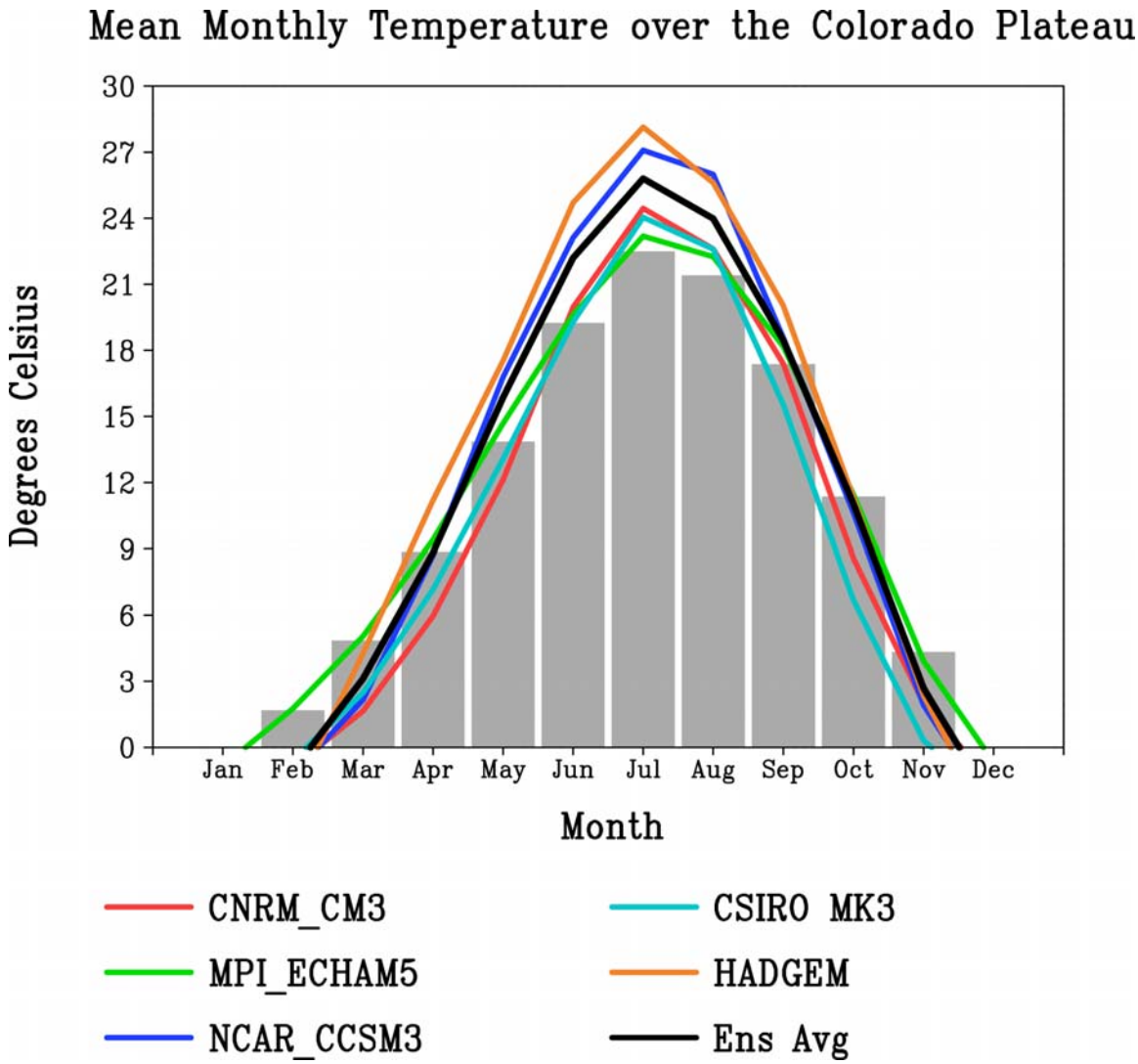
Mean Monthly Temperature over the Colorado Plateau
Degrees Celsius
30
27
24
21
18
15
12
9
6
3
0
Jan
Feb
Mar
Apr
May
Jun
Jul
Aug
Sep
Oct
Nov
Dec
Month
CNRM_CM3
CSIRO MK3
MPI_ECHAM5
HADGEM
NCAR_CCSM3
Ens Avg

Figure 4

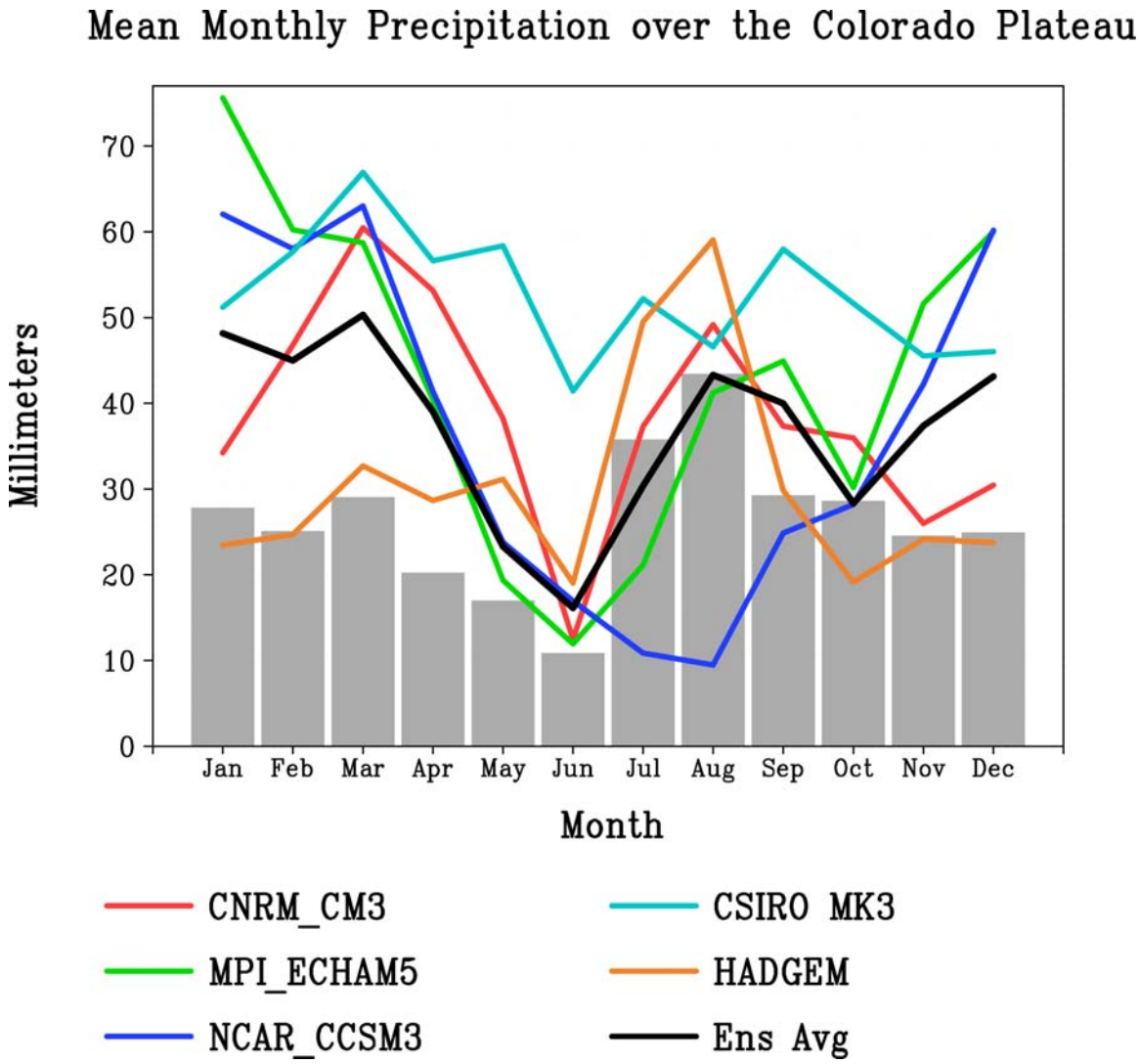
Mean Monthly Precipitation over the Colorado Plateau
Millimeters
0
10
20
30
40
50
60
70
Jan
Feb
Mar
Apr
May
Jun
Jul
Aug
Sep
Oct
Nov
Dec
Month
CNRM_CM3
CSIRO MK3
MPI_ECHAM5
HADGEM
NCAR_CCSM3
Ens Avg

Figure 5

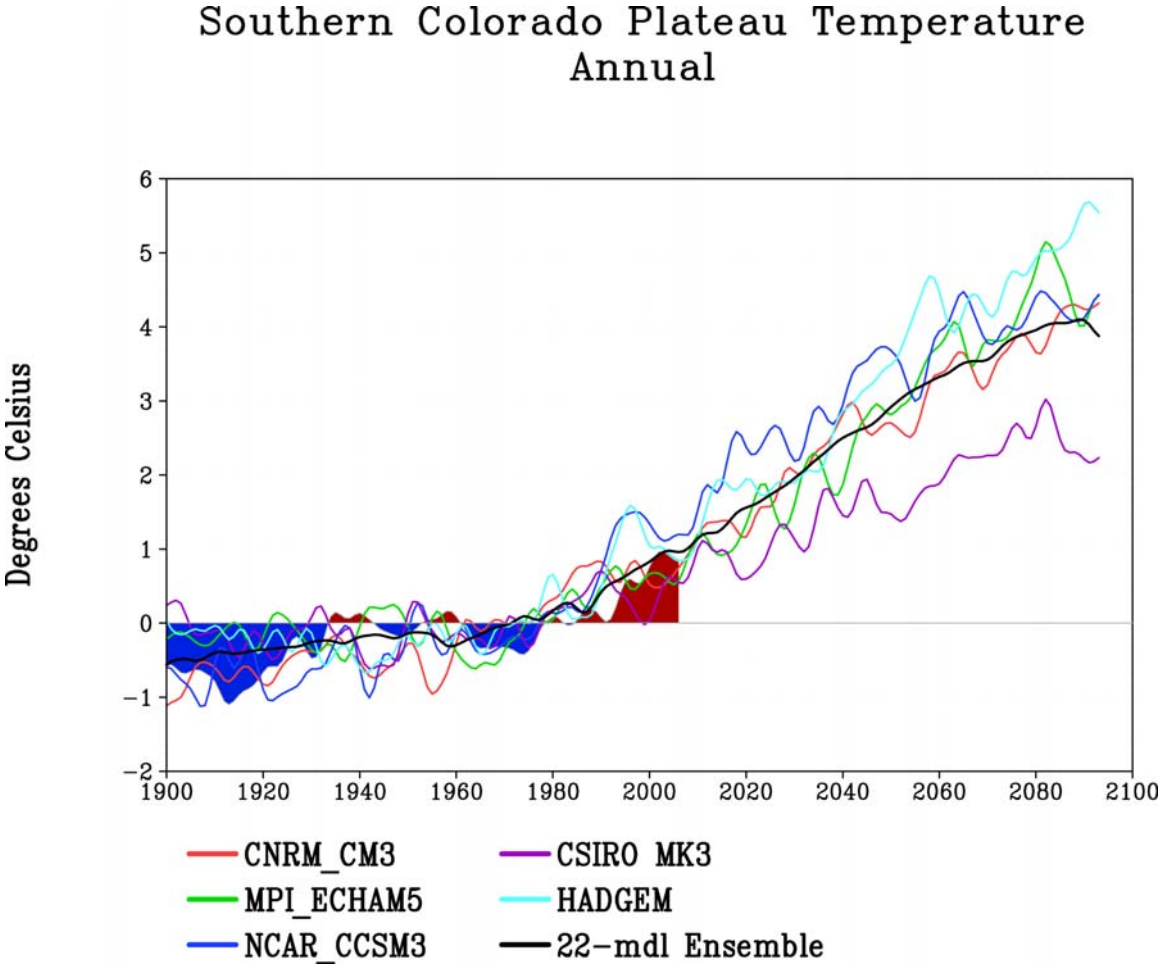
Southern Colorado Plateau Temperature
Annual
Degrees Celsius
6
5
4
3
2
1
0
−1
−2
1900
1920
1940
1960
1980
2000
2020
2040
2060
2080
2100
CNRM_CM3
CSIRO MK3
MPI_ECHAM5
HADGEM
NCAR_CCSM3
22−mdl Ensemble

Figure 6

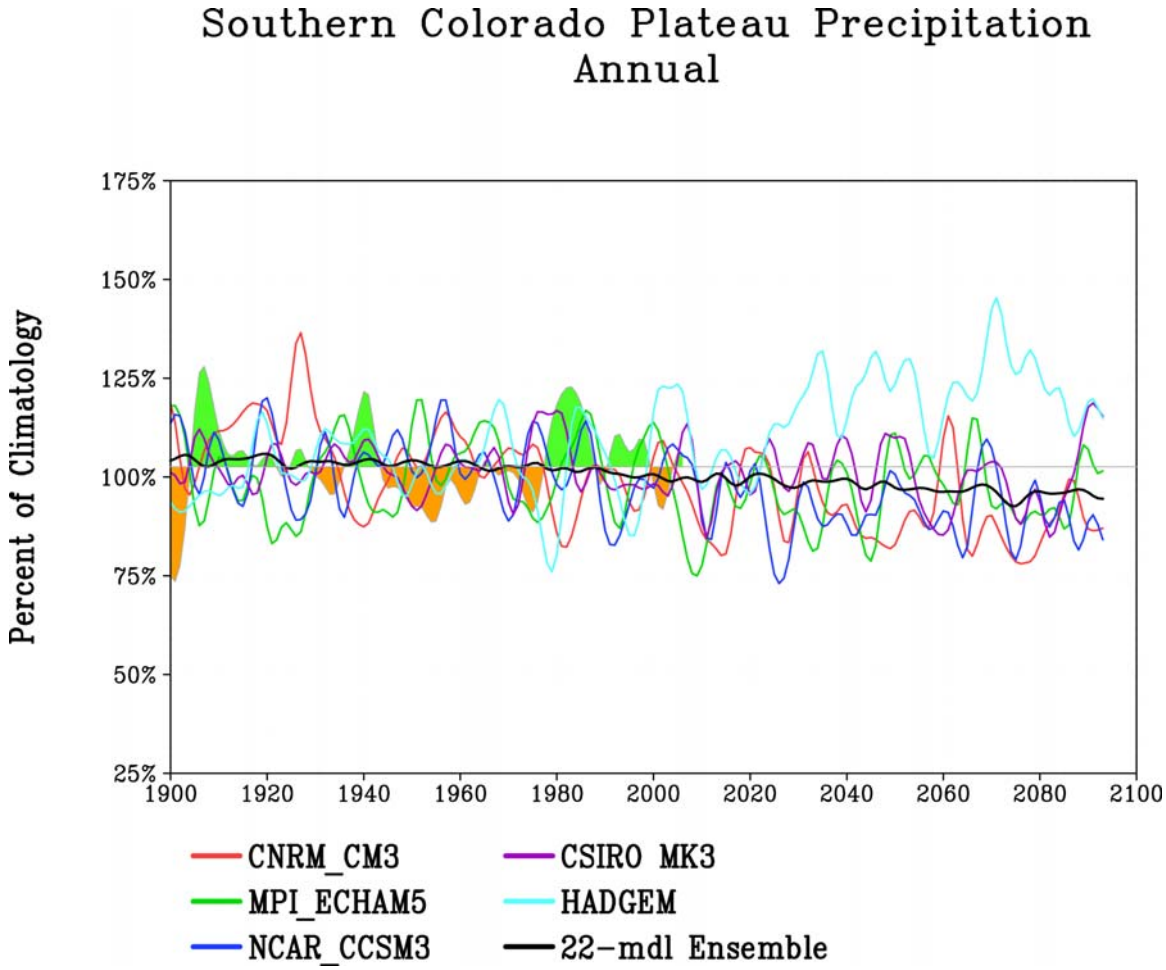
Southern Colorado Plateau Precipitation
Annual
Percent of Climatology
175%
150%
125%
100%
75%
50%
25%
1900
1920
1940
1960
1980
2000
2020
2040
2060
2080
2100
CNRM_CM3
CSIRO MK3
MPI_ECHAM5
HADGEM
NCAR_CCSM3
22-mdl Ensemble

Figure 7

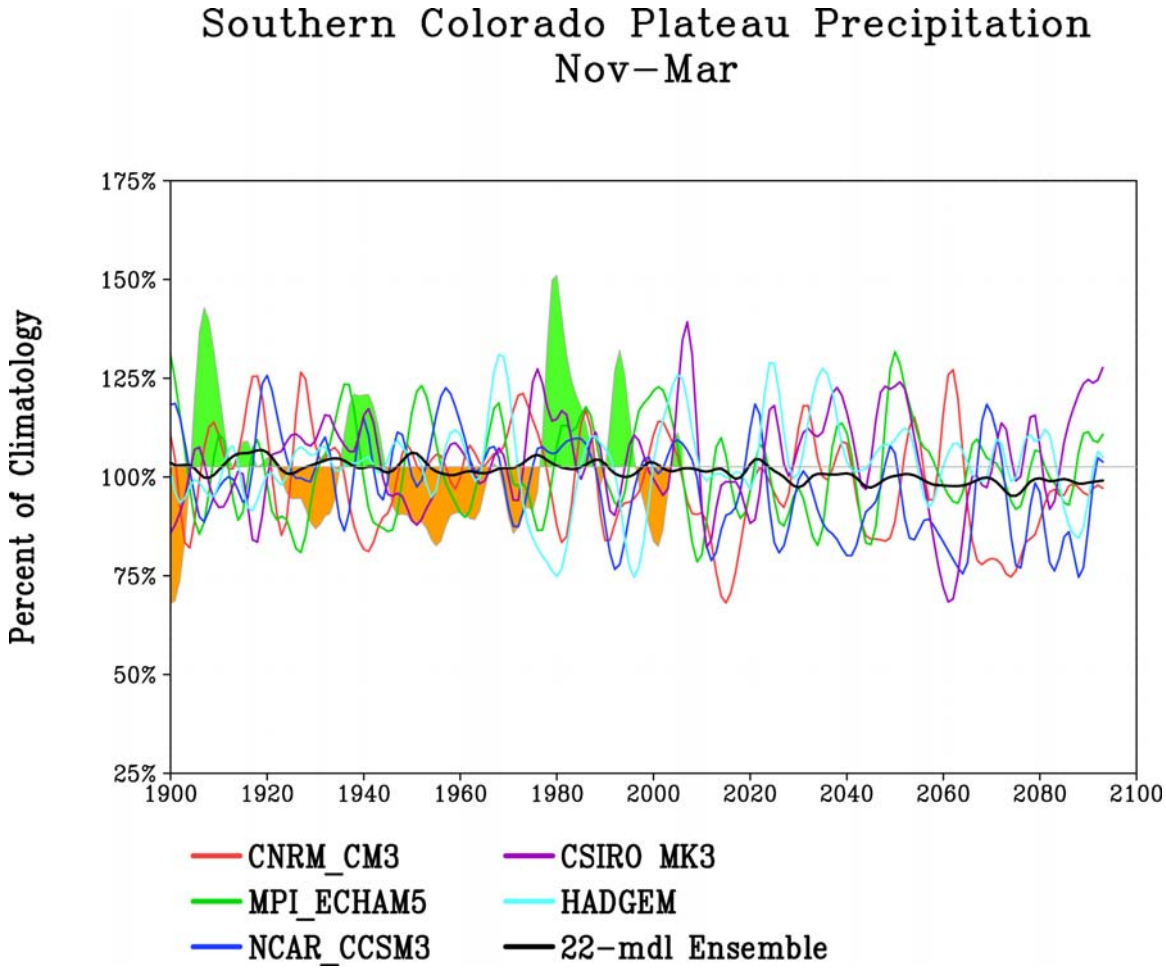
Southern Colorado Plateau Precipitation
Nov–Mar
Percent of Climatology
175%
150%
125%
100%
75%
50%
25%
1900
1920
1940
1960
1980
2000
2020
2040
2060
2080
2100
CNRM_CM3
CSIRO MK3
MPI_ECHAM5
HADGEM
NCAR_CCSM3
22–mdl Ensemble

Figure 8

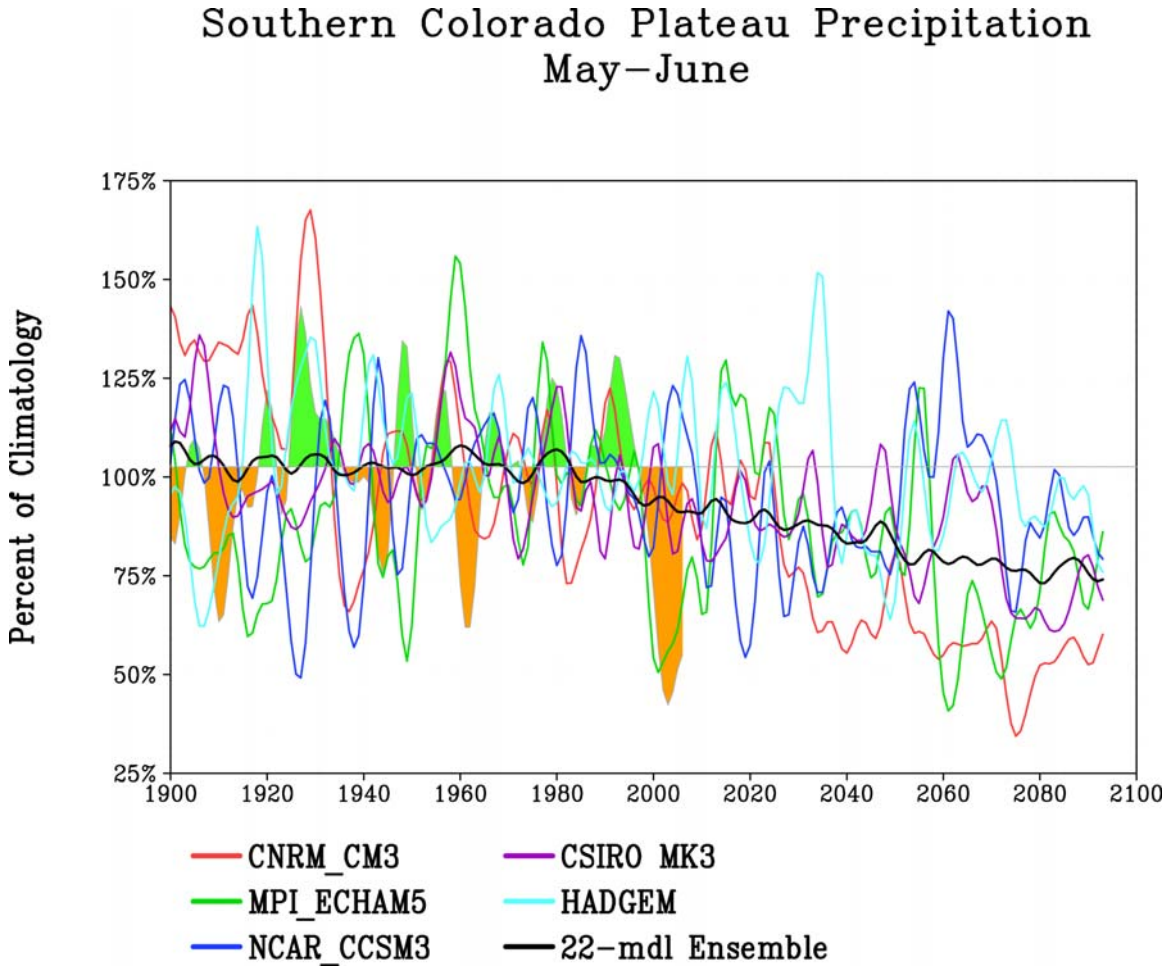
Southern Colorado Plateau Precipitation
May–June
Percent of Climatology
175%
150%
125%
100%
75%
50%
25%
1900
1920
1940
1960
1980
2000
2020
2040
2060
2080
2100
CNRM_CM3
CSIRO MK3
MPI_ECHAM5
HADGEM
NCAR_CCSM3
22–mdl Ensemble

Figure 9

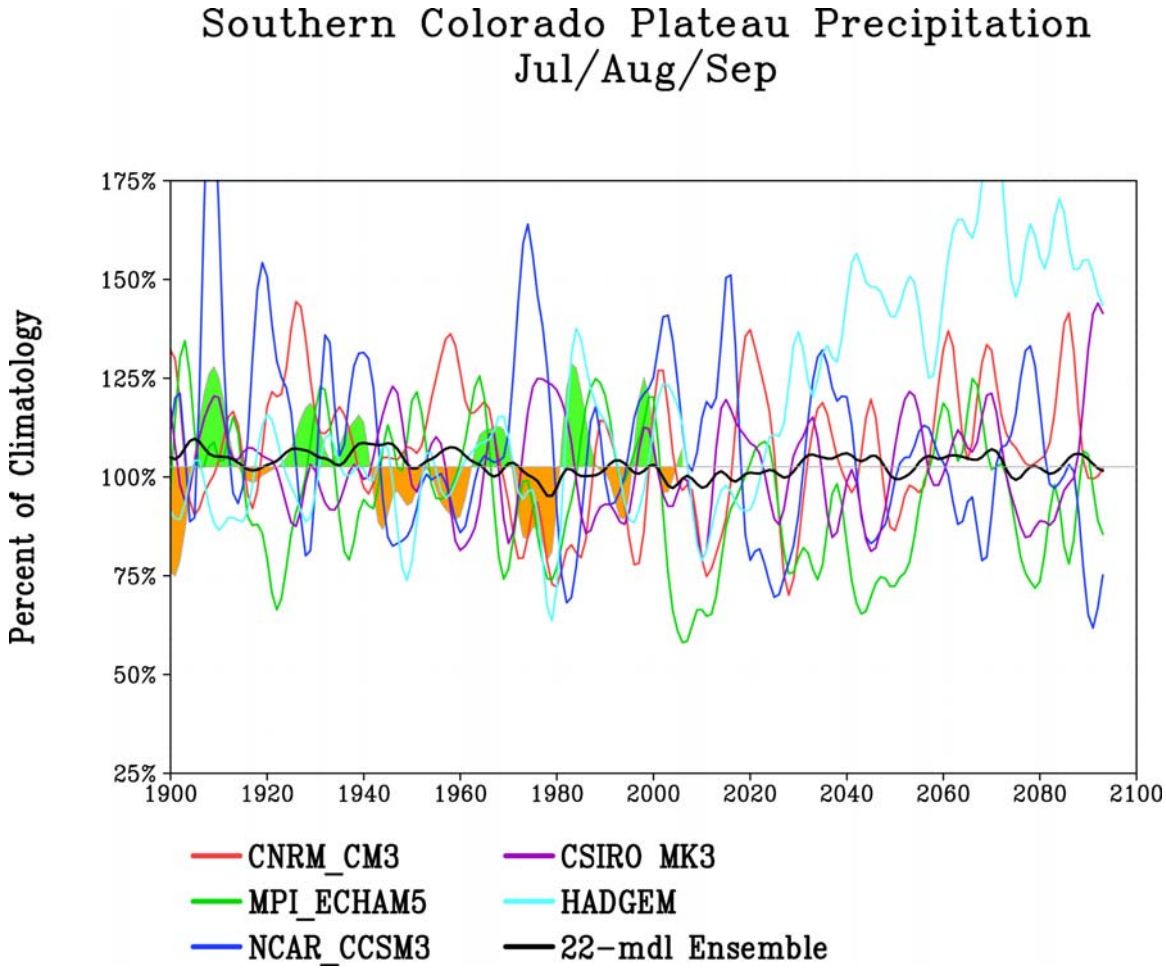
Southern Colorado Plateau Precipitation
Jul/Aug/Sep
Percent of Climatology
175%
150%
125%
100%
75%
50%
25%
1900
1920
1940
1960
1980
2000
2020
2040
2060
2080
2100
CNRM_CM3
CSIRO MK3
MPI_ECHAM5
HADGEM
NCAR_CCSM3
22-mdl Ensemble

Figure 10

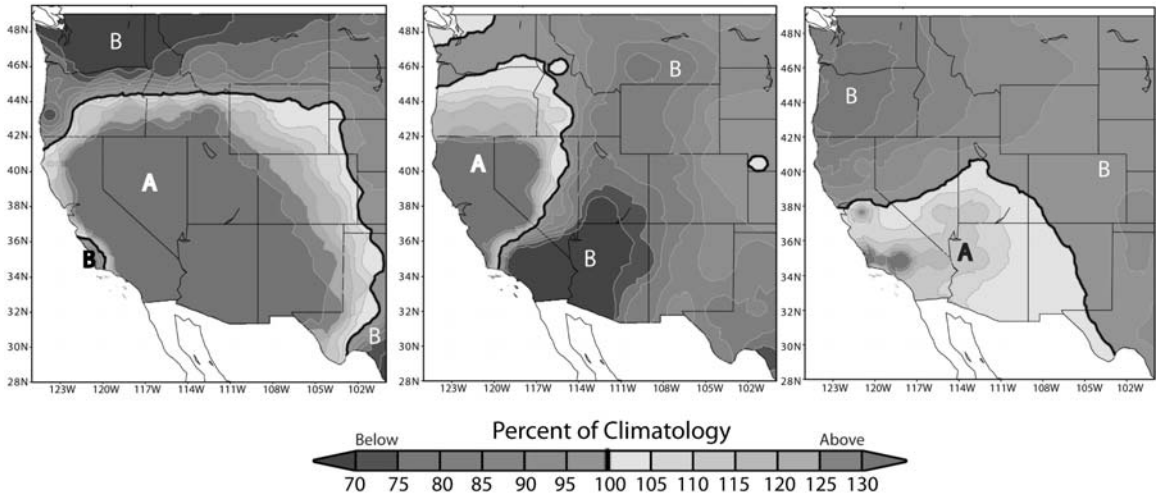
B
A
B
B
B
A
B
B
A
Below
Percent of Climatology
Above
70 75 80 85 90 95 100 105 110 115 120 125 130

Figure 11

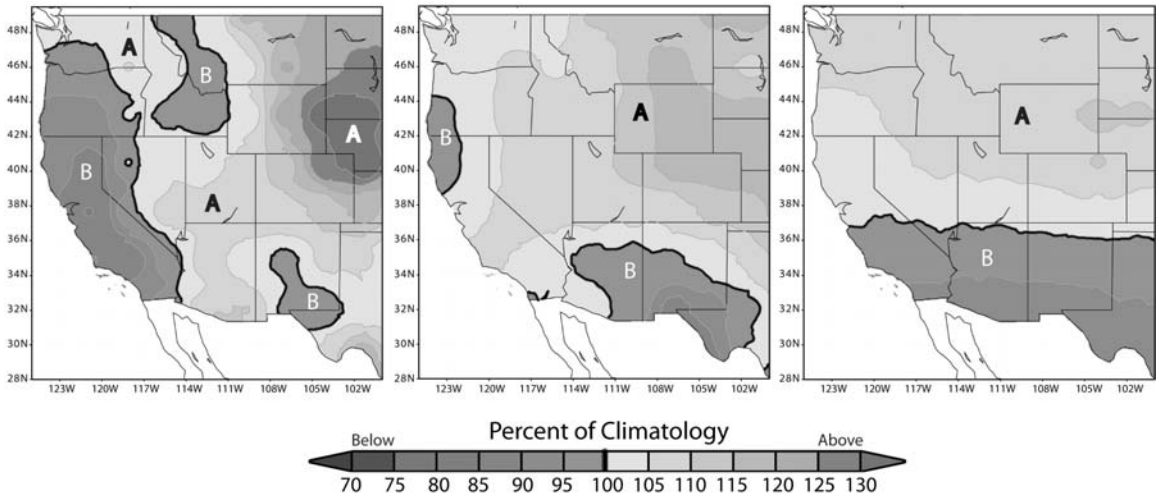
A
B
A
B
A
B
A
B
A
B
48N
46N
44N
42N
40N
38N
36N
34N
32N
30N
28N
123W
120W
117W
114W
111W
108W
105W
102W
Below
Percent of Climatology
Above
70 75 80 85 90 95 100 105 110 115 120 125 130